EXTRACTION OF INCIDENT WAVE FROM OBSERVED MOTION ON ROCK GROUND

H. Morishita (I), S. Kawamura (II)
K. Kitazawa (III), M. Hisano (III), M. Takaki (III)
Presenting Author: S. Kawamura

SUMMARY

Using the observed earthquake records at horizontal and vertical array on rock ground it was made clear that the underground motions are somewhat affected by the overlying soil layers and the motions at different points all on rock surfaces are not equal but somewhat different because of the influence. Modal damping factors of the ground were also calculated from the observed records and it was found that the value for the first mode is as large as more than 20% and those for higher modes gradually decrease. Assuming the transmission of SH waves it was tried to extract incident waves from the observed records to strip the influences of upper layers off.

INTRODUCTION

In the derivation of attenuation formulae or design response spectra from the observed earthquake motions we should be more careful how the observed motions are affected by local geological conditions. Care must be paid especially on that underground motions are somewhat or other influenced by the overlying soil layers. If it is possible to extract incident waves from the observed records, it must be effective to define the earthquake motions on free rock surface more generally, excluding the influence of the overlying layers. For this purpose it is essential to estimate rightly the physical properties of the ground. Conventionally damping ratios have often been assumed as hysteretic or viscous without enough confirmation by observed earthquake data.

INFLUENCE OF OVERLYING SOIL LAYERS ON UNDERGROUND MOTIONS

To make clear how the underground earthquake motions are influenced by the overlying soil layers analyses were done on the observed records on stiff ground as well as using one dimensional wave propagation model.

Observed and Analysed Earthquake Records

Earthquake motion measurements have been done on stiff ground by horizontal and vertical array system as shown in Fig. 1. Point No.1 is located deep in the rock, points No.2 No.5 are set on the rock surface which is covered by overlying soil layers. Point No.6 is on the ground surface.

(I) Tokyo Electric Power Company, JAPAN

(II) Senior Research Engineer, DR. Eng., Taisei Corporation, JAPAN

(III) Research Engineer, Taisei Corporation, JAPAN

The shear wave velocities of the layers are mostly more than 0.6km/sec as shown in Fig. 2. Out of nearly 200 earthquakes measured by this system five earthquakes as shown in Table 1 were selected and analysed, whose magnitudes, epicentral distances and maximum accelerations on rock surface are 3.9∿5.4, 32∿164km and 3.0∿10.0 Gal respectively.

Comparison between Observed Motions on Rock Surface

Fourier amplitude ratios were calculated of the points No.3∿No.5 on the rock surface and point No.6 on the ground surface to the point No.2 on the rock surface which is looked as a standard for this analysis. Average ratios of five earthquakes are shown in Fig. 3. Compared with the remarkable peak at about 10Hz found in the ratio No.6/No.2 only slight undulations can be seen in the ratios of No.3, No.4 and No.5 to No.2. This indicates that the motions at different points all of which are on rock surface and not so distant to each other are similar compared with the amplification in the vertical array. However the undulations observed in the ratios of rock surface points are quite different to each other, which indicates that the motions on rock surface are not same but somewhat different. Table 2 is the analytical natural frequencies of the soil layers overlying each rock surface point, which are identified also in Fig. 3. The tendency can be seen in Fig. 3 that the ratio spectrum is dipping at the natural frequencies of the layers overlying each divided point and jutting at the natural frequencies of the layers overlying point No.2. It can be pointed out that these phenomena might be due to the influence of the overlying soil layers.

One Dimensional Wave Propagation Analysis

Transfer function of incident wave/observed wave at the point No.2 was calculated using one dimensional wave propagation model. The soil and rock layers above the point No.1 were modeled into 13 layers whose damping factors were assumed as Maxwell-type visco-elastic damping with the value h=0.28 for the first natural frequency 1.56Hz of the soil column above the point No.1. The damping value was derived from the spectrum fitting analyses described afterwards. As shown in Fig. 4 the amplitude ratio is not unity but fluctuates around unity, which indicates that the observed motion is not the same as the incident wave but distorted. The peak frequencies of the overlying soil layers are shown in Table 2. This is because the motion of the point is suppressed at these frequencies. Even if the incident wave is common to each point on rock surface the observed motions become different to each other due to the difference of upper soil layers.

DAMPING FACTORS OF STIFF GROUND

As shown previously the observed underground motions are somewhat influenced by the overlying soil layers. Then it might be erroneous to derive the characteristics of the motion on free rock surface directly from these underground observed records. To avoid the defects it would be effective if the incident wave is able to be extracted from the observed records. For this purpose analytical procedure is necessary, where physical properties should be decided appropriately. The densities and shear wave velocities can be specified rationally from the test data. But in most

cases damping factors have been only assumed as hysteretic or viscous with little confirmation by observed earthquake data.

Modal Damping Factors by Lumped Mass Models

Using the lumped mass models of the soil column modal damping factors were calculated by the spectrum fitting method whose flow chart is shown in Fig. 5. Two lumped mass models were used to represent the surface layers above the point No.2 and the total layers above the point No.1, which were named "surface model" and "total model" respectively. Both models are fixed at their bottom and observed accelerations were input for the response analyses. Natural frequencies of both models are compared with the observed predominant frequencies in Table 3, where good correlations can be seen. The damping factors obtained by the spectrum fitting method are plotted versus frequency in Fig. 6. The damping factor for the first mode is as large as more than 20% and those for higher modes are less than that with conspicuous decrease against the increase of frequency. Fig. 7 shows the simulated transfer functions as compared with the observed ones.

Element Damping Factors by Visco-Elastic Models

To account for the decreasing characteristics of modal damping factors in higher modes by visco-elastic element model viscous or hysteretic type of model is inappropriate. Because the modal damping factors by those models are frequency proportional or constant independent of frequency. Instead of them Maxwell type or Maxwell-hysteretic hybrid model will be suitable.

TRIAL OF EXTRACTION OF INCIDENT WAVES

The extraction of incident waves from the observed accelerograms was tried by lumped mass models as well as by one dimensional wave propagation theory. Here the propagation of plane SH waves in the upright vertical direction was assumed.

Extraction of Incident Wave by a Lumped Mass Model

A lumped mass model is made to represent the soil column where earthquake motion measurements are done at its bottom and on the surface. The base of the model is fixed. Base shear stress time history is calculated by inputting the observed acceleration at the base, when the modal damping factors obtained by the spectrum fitting method are used to simulate the response of the soil column as correct as possible. This base shear stress time history is applied to the dashpot with the damping coefficient of wave impedance as equation (1) to obtain the velocity response.

$$C = \rho \cdot Vs \cdot A \quad \ldots\ldots\ldots \quad (1)$$

where C: Damping Coefficient, ρ: Density of Bed Rock,
Vs: Shear Wave Velocity of Bed Rock, A: Area of Soil Column
The velocity response is differentiated by the Fourier transformation to obtain acceleration which corresponds to (dissipative wave - incident wave).

Then by subtracting this acceleration from the observed acceleration which was used as the input wave, twice of the incident wave can be obtained. The concept of this procedure is shown in Fig. 8 .

Extraction of Incident Wave by a Wave Propagation Model

The transfer function of incident wave/observed wave can be calculated by one dimensional wave propagation model as shown in Fig. 4. By multiplying the Fourier function of the observed wave by this transfer function in frequency domain the Fourier function of the incident wave can be calculated. Then Fourier inverse transformation is operated and the time history of the incident wave can be obtained.

The Results of Extraction

Extracted incident waves at the points No.2 ∿ No.5 on the rock surface using lumped mass models are shown in Fig. 9 . The waves were expected to resemble each other, but actually it was not realized. No.2 and No.4 are similar, but No.3 and No.5 are different from these two. Maximum accelerations of the incident and observed waves are listed in Table 4. The acceleration ratios of incident waves to the observed ones are about 0.7. The incident wave at the point No.2 extracted by the wave propagation model is shown in Fig.10 along with the observed wave. The two extracted incident waves and the observed one are similar to each other. The maximum acceleration of the incident wave by the lumped mass model is a little smaller than that by the wave propagation modal, which may be due to the difference of damping factors in higher modes. Fig. 11 is the Fourier amplitude ratios of the observed and incident waves at the points No.3 ∿ No.5 divided by those of No.2. Though the ratios of the incident waves were expected to become closer to unity than those of the observed waves, they were quite different. This may be due to the reflection of the dissipative waves at the lower boundaries than those considered in this analyses, and the mixture of the waves other than SH waves.

CONCLUSIONS

As the results of the analyses of the underground earthquake motions following conclusions were introduced.

1) The underground motions are influeced by the overlying soil layers. It is better to take the effects off from the underground motions in the derivation of the seismic characteristics on free rock surface using those data.
2) The modal damping factors of the stiff ground analysed herein are as large as more than 20% for the first mode and gradually decrease in higher modes. The decreasing tendency in higher modes can be expressed by Maxwell or Maxwell-hyteretic visco-elastic model.
3) Extraction of incident waves from the observed data would be effective to take the influence of upper layers off. Two methods (lumped mass model and wave propagation model) can be used for the purpose, where physical properties, especially damping factors, should be rationally decided.
4) The results of the trial of the extraction of incident waves here mentioned were not so good as to satisfy the expection.

The waves other than SH waves and the geological conditions more below might have affected the results.

ACKNOWLEDGEMENT

The earthquake records were obtained by the Research Committee of Strong Earthquake Instrument Arrays on Rock Site (Chairman: Dr. Shun-ichiro Omote).

Table 1 Analysed Earthquakes

Eqk. No.	Date	Epicenter	Depth (km)	M	Δ (km)	Max.Acc. (Gal)
85	1979.06.22	West of Tokyo	0	3.9	32	3.0
89	07.02	S.W. of Ibaragi	60	4.1	52	4.6
123	10.09	S.W. of Ibaragi	50	4.1	44	4.7
139	11.25	Off Coast of Ibaragi	90	5.4	164	6.8
156	1980.02.02	North of Kanto	50	4.2	43	10.0

M: Magnitude , Δ: Epicentral Distance
Max.Acc.: Maximum Acceleration on Rock Surface

Table 2 Analytical Natural Frequencies of Overlying Soil Layers

(Hz)

Mode	Point			
	No.2	No.3	No.4	No.5
1st	3.28	2.52	3.73	3.26
2nd	9.48	6.48	9.43	7.37
3rd	14.1	10.4	15.1	12.9

Table 3 Comparison of Analytical and Observed Frequencies

(Hz)

		1st	2nd	3rd	4th	5th	6th
Total	Obsvd.	1.51	4.55	7.30	9.90	12.7	14.8
Model	Analt.	1.56	4.68	7.80	10.1	12.8	14.5
Surface	Obsvd.	3.20	9.15	-	-	-	-
Model	Analt.	3.28	9.48	14.1	-	-	-

Table 4 Maximum Accelerations of Incident and Observed Waves

Point	Max.Acc.(Gal)		Ratio
	Incident	Obsreved	Inc./Obs.
No.2	1.95	2.68	0.73
No.3	1.49	1.89	0.79
No.4	1.83	2.60	0.70
No.5	1.93	3.33	0.58
Average	1.80	2.63	0.70
Standard Deviation	0.15	0.34	0.05

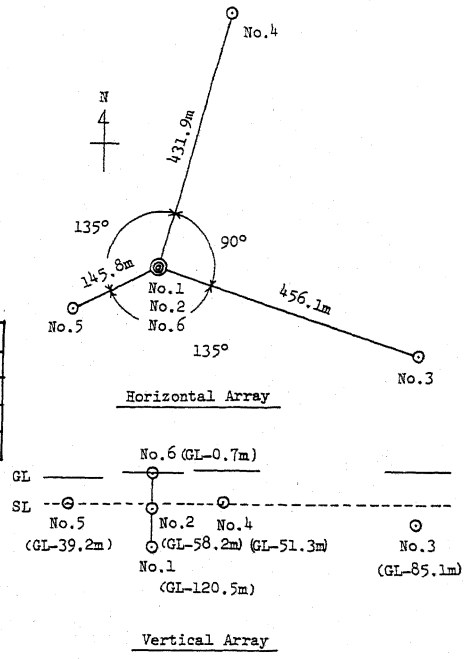

Fig.1 Horizontal & Vertical Array

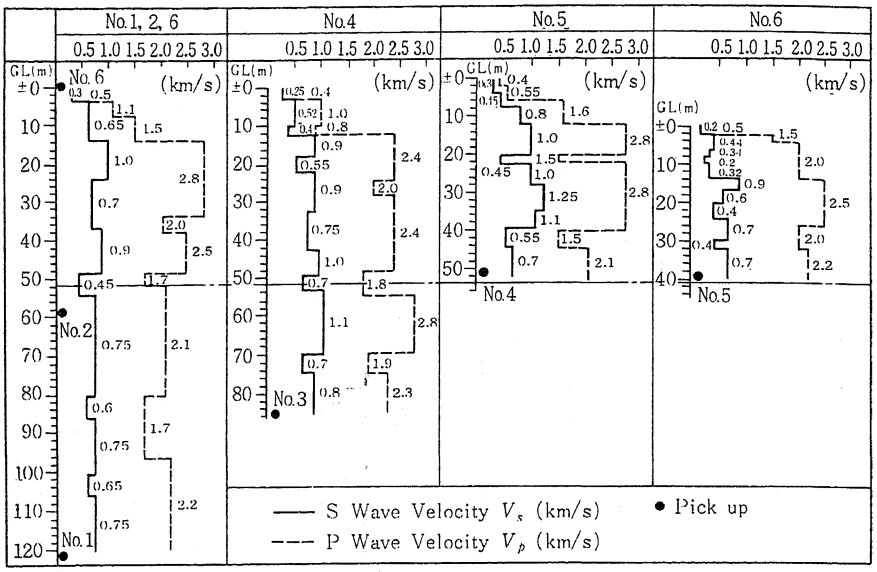

Fig.2 Elastic Wave Velocities of the Soil & Rock Layers

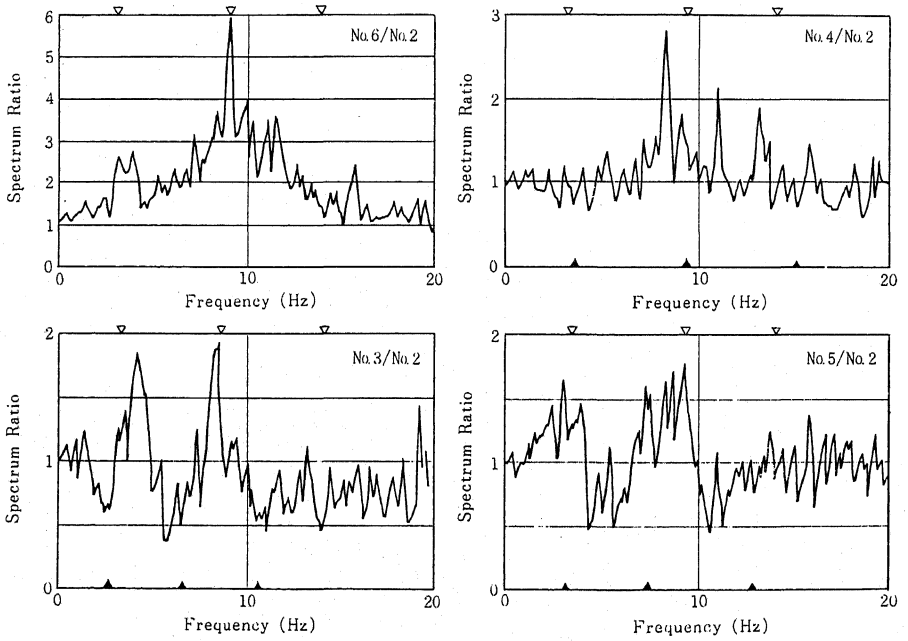

Fig.3 Average Fourier Amplitude Ratios

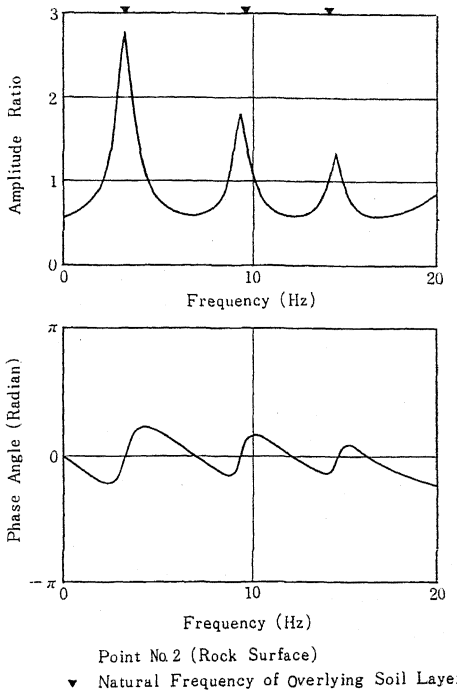

Fig.4 Analytical Transfer Function Incident Wave/Observed Wave

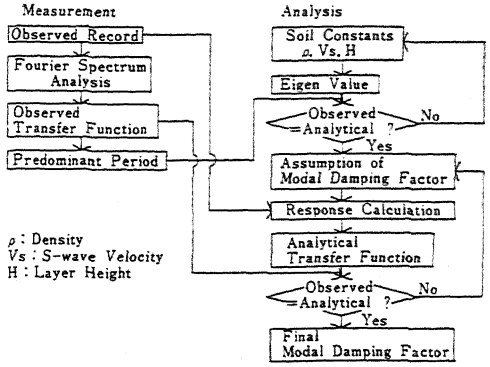

Fig.5 Spectrum Fitting Method

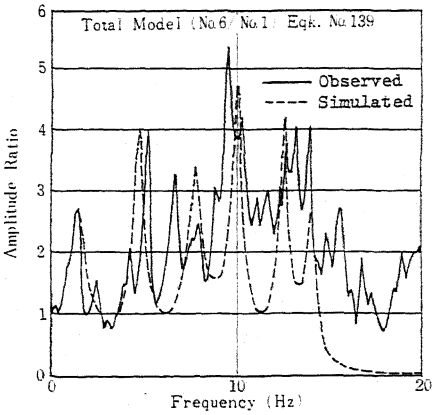

Fig.7 Simulated Transfer Function

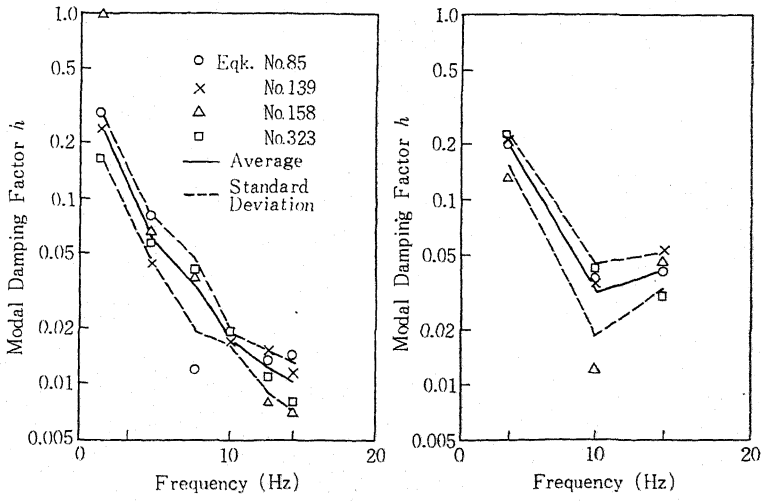

(a) Total Model No.6/No.1 (b) Surface Model No.6/No.2

Fig.6 Modal Damping Factors vs. Frequency

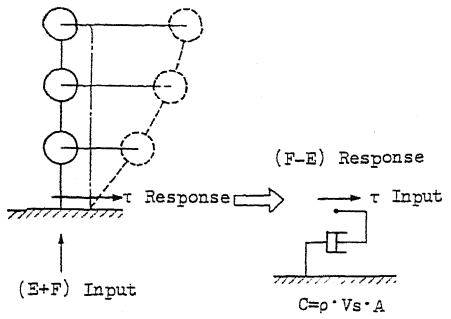

E:Incident Wave, F:Dissipative Wave,
τ:Shear Stress, C:Damping Coefficient,
ρ:Density, Vs:Shear Wave Velocity,
A:Area of Soil Column

Fig.8 Extraction of Incident Wave by a Lumped Mass Model

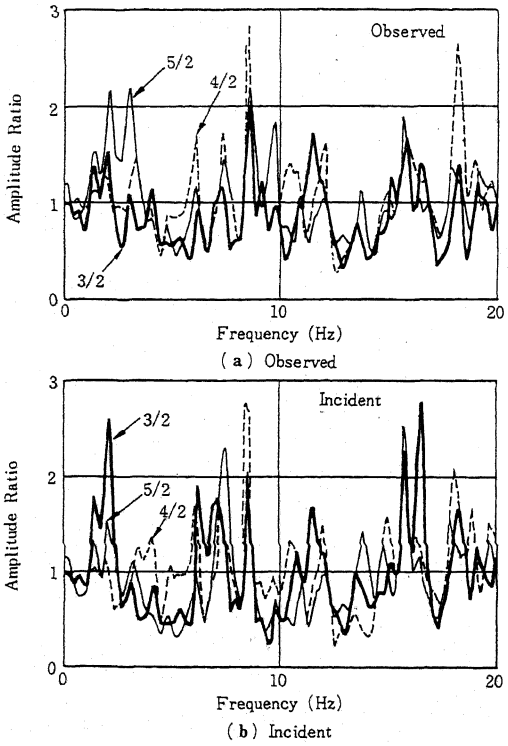

Fig.11 Fourier Amplitude Ratios of the Observed and Incident Waves on Rock Surface

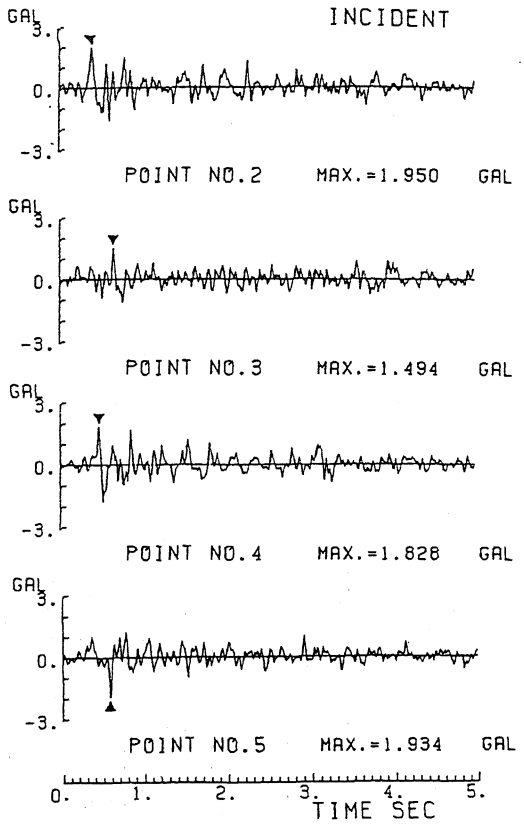

Fig.9 Extracted Incident Waves by Lumped Mass Models

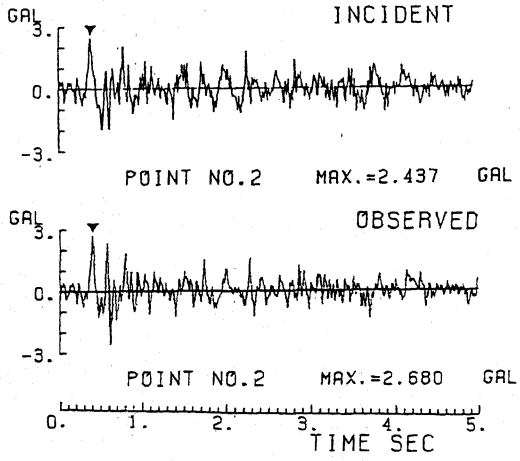

Fig.10 Extracted Incident Waves by Wave Propagation Model and the Observed Wave